Optimal Design and Implementation of an Omnidirectional Panel Speaker Array Using the Genetic Algorithm

Mingsian R. Bai
e-mail: msbai@mail.nctu.edu.tw

Jihting Kuo

Department of Mechanical Engineering,
National Chiao-Tung University,
1001 Ta-Hsueh Road, Hsin-Chu 300, Taiwan,
ROC

A panel speaker array with omnidirectional radiation pattern is presented in this paper. Array signal-processing techniques are utilized to manipulate the sound beam electronically such that wide-angle radiation can be maintained over a large frequency range. In order to achieve this purpose without sacrificing the array efficiency, the genetic algorithm (GA) is employed in the design stage to calculate the optimal array coefficients. The GA proved to be an effective technique in searching for the array coefficients that maximize the efficiency with desired flatness of radiation pattern. In addition, a modified design is also proposed to further enhance the efficiency in the low frequency range. The resulting designs are implemented on a digital signal processor platform and experimentally verified by using a small 5×1 panel speaker array and a large 3×3 panel speaker array. [DOI: 10.1115/1.1805004]

1 Introduction

This paper focuses on the development of a panel speaker array with omnidirectional radiation pattern. This array serves as a projection screen of an audio and video system that integrates the technologies of panel speakers, video projection, and array signal processing. This system is intended for applications such as oral presentation, home theater, conferencing, public addressing, and so forth.

The main reason of using panel speakers lies in their flatness and compactness, which makes them well suited for the application, such as the projection screen, in our case. However, the randomly distributed flexural modes of a large panel create efficiency problems in low frequency and peculiar directivity in high frequency [1]. A possible solution to these problems associated with panel speakers is to break a large panel into smaller pieces and excite each element independently, using array signal-processing techniques. This approach enables us to ''control'' the beam pattern of the generated sound field with more flexibility over the conventional single panel configuration. In particular, we seek in this work to generate an omni directional response over a wide frequency range using panel speaker arrays.

Figure 1 shows a linear speaker array and its signal processing unit. For a uniformly linear array, it is well known that the directional response is the spatial Fourier transform of the array coefficients [2]. It is then straightforward to obtain a frequency-invariant, omnidirectional array by using inverse Fourier transform. However, the omnidirectionality is generally achieved at the expense of array efficiency. The array coefficients resulting from inverting perfect spectral flatness tend to be an impulse function in the spatial domain, which implies only one element in the array is active and the remaining elements are at rest. Instead of the above naïve approach, a method of optimization was employed in this paper to calculate the array coefficients that attain optimal efficiency with a desired directional response, or spectral flatness in the transformed domain. Due to the highly nonlinear nature of the array optimization problem, this study employs an optimization technique, the genetic algorithm (GA), to effectively search the global optimum in a nonlinear space with a large number of parameters. Typically, there are $2(2N+1)$ parameters, including the magnitudes and phases, to determine for an array with $2N+1$ elements. Thus, the search space can be very large for a moderate number of array elements. The GA is well suited for dealing with such optimization problems. Reference [3] optimized a linear array and a planar array using GA to produce beam patterns with the lowest side-lobe level. Reference [4] also proposed a design technique for linear array using optimization methods. As opposed to the optimization-based approaches, Ref. [5] suggested an array design method that does not yield optimal, but reasonable results, while the analytical solution guarantee a certain amount of control that is not present when an optimization method is used.

This paper proposes a GA-based technique for finding array coefficients to maximize two cost functions: spectral flatness and array efficiency. Admittedly, the motivation of this research comes to some extent from [5], where array efficiency and spectral flatness were achieved in an analytical manner with real coefficients. However, the present research differs from [5] in that complex coefficients are employed in the design to provide more degrees of freedom than real-coefficient design during the optimization process. However, this set of complex coefficients applies to one frequency only. The same procedure must be repeated to gather sufficient frequency samples for designing time domain array filters. The details of the design procedure will be presented in the following sections. In addition to the basic version, a modified design is also proposed to further enhance the efficiency in the low frequency range, where the design effort can be shifted from the ''invisible'' region to the ''visible'' region. These two optimal designs are referred in this paper as the omnidirectional array and the modified omnidirectional array.

In order to verify the proposed optimal array designs, experiments were carried out in this research. A small 5×1 panel speaker array and a large 3×3 panel speaker array were constructed for experimental verification. Signal processing and electronic compensation are carried out by using a multichannel digital signal processor (DSP). Results obtained using the optimal designs will be discussed with reference to an uncompensated array.

Contributed by the Technical Committee on Vibration and Sound for publication in the JOURNAL OF VIBRATION AND ACOUSTICS. Manuscript received August 2002; final revision March 2004. Associate Editor: Richard F. Keltie.

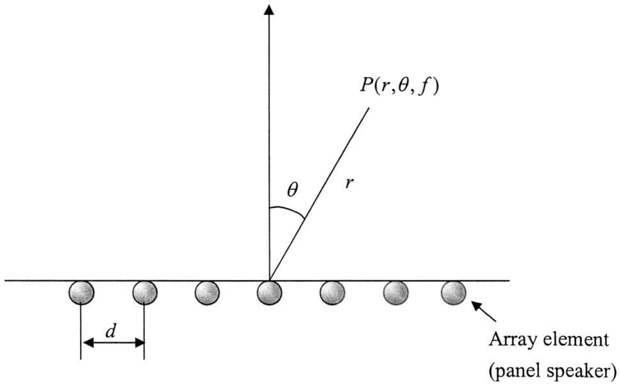

(a)

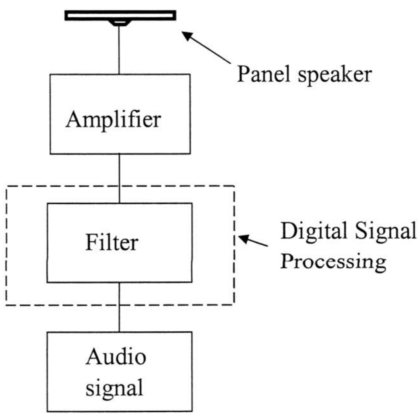

(b)

Fig. 1 A linearly uniform linear array. (*a*) The schematic of a panel speaker array, (*b*) the signal processing unit of the panel speaker array

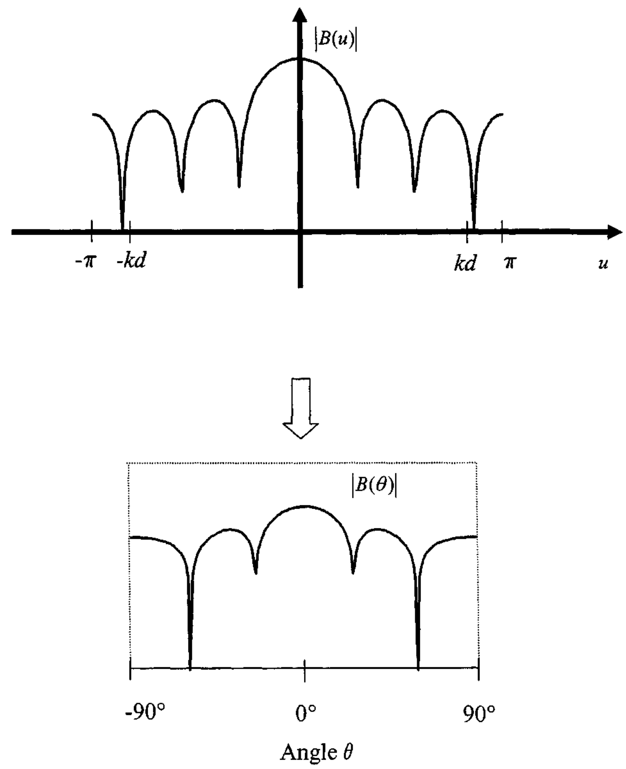

Fig. 2 Beam pattern of a ULA plotted against the dimensionless angle *u* and the look angle *θ*

2 Fundamentals of Uniformly Linear Arrays

The array configuration employed in this work is the uniformly linear array (ULA) in which array elements are equally spaced in a straight line. Some fundamentals of ULA relevant to the ensuing discussion are given in this section.

2.1 Far-Field Model of a ULA. Consider the ULA with $2N+1$ elements, as shown in Fig. 1(*a*). The observation point is assumed in the far-field such that $r \gg 2Nd$, where d is the spacing between two adjacent elements and r is the distance between the observation point and the array center. As a rule of thumb, the far field begins at the distance three times the characteristic dimension of the source [4] or, in our case, $2Nd$. The sound pressure of this array is given by [5]

$$P(f,\theta,r)=A(f,\theta)R(f,r)B(f,\theta) \tag{1}$$

where f is the frequency of the source, θ is the angle measured from the normal of the array, $A(f,\theta)$ is the directional response of a single array element, and $R(f,r)=r^{-1}\exp(j2\pi fr/c)$ represents the spherical spreading. The beam pattern $B(f,\theta)$ is expressed as

$$B(f,\theta)=\sum_{n=-N}^{N} g_n(f)e^{jn(2\pi fd\sin\theta/c)} \tag{2}$$

where $g_n(f)$ is the array coefficient of the nth element and c is the speed of sound.

We further restrict the array coefficients $g_n(f)$ to be frequency-independent complex constants g_n. Then the beam pattern can be written as

$$B(u)=\sum_{n=-N}^{N} g_n e^{jnu} \tag{3}$$

where the dimensionless angle $u=kd\sin\theta=2\pi fd\sin\theta/c$; k being the wave number, d being the interelement spacing, f being the frequency, and c being the speed of sound. Inspection of Eq. (3) reveals that the beam pattern is essentially the frequency response of a FIR filter with coefficients g_n. Thus, the design problem of an omnidirectional array can be regarded as the design of an all-pass FIR filter.

2.2 Charateristics of a ULA. Analogous to time-domain filters, a ULA is a filter in the spatial domain, where the wave number k is the spatial frequency, the spacing d is the spatial sampling period, and the nondimensional angle u is the digital spatial frequency. Increase of the array aperture will result in the decrease of the beam width and thus improved resolution.

The beam pattern of a typical ULA is shown in Fig. 2. The nondimensional angle $u=2\pi fd\sin\theta/c$ is a nonlinear function of the look angle θ. The *beam-broadening effect* arises as θ varies from 0 deg to ± 90 deg. When the main beam of an array is steered to θ_0, its beam width can be approximated as [2]

$$2\Delta\theta \approx 2\frac{\lambda_c}{(2N+1)d\cos\theta_0} \tag{4}$$

where $\Delta\theta$ is the angle difference between the look angle θ_0 and the adjacent null point and λ_c is the source wavelength.

The physical limits of the look angle $\theta=\pm 90$ deg correspond to the dimensionless angle $u_0=\pm kd$ for specific wave number k and interelement spacing d, which in turn increases with increasing frequency f. Note that the parameter u_0 is then likely to be greater than π above a certain frequency. In this case, grating

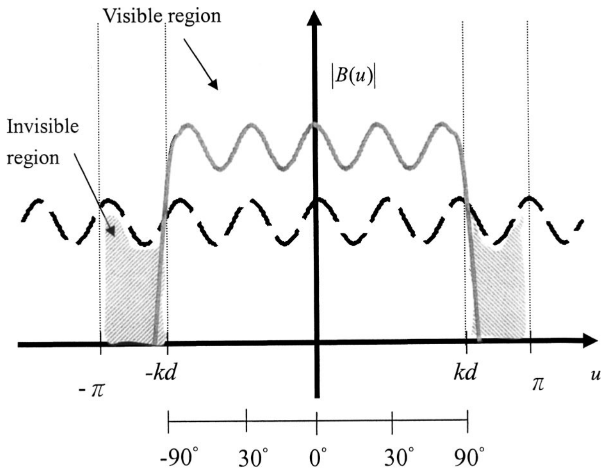

Fig. 3 The full band design and the bandpass design for the omnidirectional array. Solid line represents bandpass beam pattern, dashed line represents full band beam pattern

lobes will appear within the observation range. To avoid the grating lobes, the spacing d is generally chosen according to

$$d \leqslant \frac{\lambda}{2} \tag{5}$$

where $\lambda = c/f$ is the wavelength and c is the speed of sound.

2.3 Omnidirectional Response. As mentioned previously, the goal of this work is to design speaker arrays with omnidirectional characteristics. Some considerations with regard to this aspect are addressed as follows. The dashed line in Fig. 3 shows a typical omnidirectional beam pattern plotted in the u-domain. The smaller the ripples are, the closer the array is to the ideally omnidirectional response. Since the parameter u is dimensionless, the omnidirectional response applies to all frequencies.

The array efficiency can be enhanced by a further modification to the directional response design. With reference to Fig. 3, in sufficiently low frequency, it could happen that the effective range at which the look angle θ falls within the range $[-\pi/2,\pi/2]$ corresponds to a nondimensional critical angle less than π (i.e., $u_0 = kd\,\sin(\pi/2) = kd < \pi$). The regions $[-\pi,-kd)$ and $(kd,\ \pi]$ are physically "invisible." Therefore, it would be a waste to provide energy in the invisible regions (shadow areas) during the design process because in those regions no sound radiation will physically exist. Alternatively, it is more desirable to design a bandpass array pattern (solid line in Fig. 3), concentrating within the "visible" region $[-\pi,\pi]$, such that the overall efficiency can be improved. In Section 3, a phase-compensation scheme will be presented to produce an omnidirectional pattern, while at the same time to prevent the design effort from being wasted in the invisible region.

3 Optimization Schemes for Omnidirectional Arrays

In this section, optimization schemes are presented that are aimed at achieving a better compromise between array efficiency and the omnidirectional response for the panel speaker array.

3.1 Preliminary Scheme. Let the autocorrelation function be

$$R(k) = \sum_{n=-\infty}^{\infty} g_n g_{k-n}^{*} \tag{6}$$

where g_n is the array gain for the nth element and $*$ denotes complex conjugate [6]. The power spectrum is given by

$$S(u) = |B(u)|^2 = B(u)B^{*}(u). \tag{7}$$

It can be shown the following relations are valid

$$g_n \overset{FT}{\leftrightarrow} B(u)$$

$$R(k) \overset{FT}{\leftrightarrow} S(u),\ \ S(u) = B(u)B^{*}(u)$$

$$C(k) \overset{FT}{\leftrightarrow} S^2(u),\ \ S^2(u) = S(u)S^{*}(u)$$

where

$$C(k) = \sum_{n=-\infty}^{\infty} R(n)R^{*}(k-n)$$

and FT denotes the Fourier transform. Thus, by the above Fourier relations

$$S^2(u) = \sum_{k=-\infty}^{\infty} C(k)e^{jku}. \tag{8}$$

It is well known that the power spectrum is the Fourier transform of the autocorrelation function

$$S(u) = \sum_{k=-\infty}^{\infty} R(k)e^{-jku}. \tag{9}$$

Assume the array consists of $2N+1$ elements. The first performance index employed in the optimization procedure is the "array efficiency"

$$\eta = \frac{R(0)}{(2N+1)\max|g_n|} \tag{10}$$

where $\mathbf{g} = \{g_n | -N \leqslant n \leqslant N, n \in N\}$, and

$$R(0) = \sum_{n=-N}^{N} |g_n|^2 = \frac{1}{2\pi}\int_{-\pi}^{\pi} S(u)du \tag{11}$$

where the Parseval theorem has been invoked. Thus, the array efficiency can be interpreted as the mean-square spectrum normalized by $\max|g_n|$. The array efficiency will be close to unity if all array elements are quite active.

Using Eq. (9), we have

$$\frac{1}{2\pi}\int_{-\pi}^{\pi} S(u)du = \int_{-\pi}^{\pi}\sum_{k=-2N}^{2N} R(k)e^{jku}du = R(0). \tag{12}$$

By the Parseval's relation,

$$\sum_{k=-2N}^{2N} |R(k)|^2 = \frac{1}{2\pi}\int_{-\pi}^{\pi} S^2(u)du. \tag{13}$$

Define the "merit factor" as [7]

$$F_a = \frac{R^2(0)}{\sum_{k\neq 0} |R(k)|^2}. \tag{14}$$

The interpretation of the merit factor follows from substituting Eqs. (12) and (13) into Eq. (14)

$$F_a = \frac{\left(\int_{-\pi}^{\pi} S(u)du\right)^2}{2\pi\int_{-\pi}^{\pi}[S^2(u) - R^2(0)]du} \tag{15}$$

where the denominator of F_a can also be written as the spectral variance, or the measure of flatness

$$v_f \triangleq \sum_{k\neq 0} |R(k)|^2 = \int_{-\pi}^{\pi} [S^2(u) - R^2(0)]du$$

$$= \int_{-\pi}^{\pi} [S(u) - R(0)]^2 du. \quad (16)$$

Thus, the merit factor F_a can be interpreted as the ratio of the mean-square spectrum over the spectral variance. The mean-square spectrum can be related to the efficiency of the array, whereas the spectral variance can be related to the spectral flatness. It is then most desirable to have an array with a large merit factor, i.e., high efficiency and small variance. However, there is generally a tradeoff between these two indices, which entails for the need of an optimization procedure to best accomplish this tradeoff.

3.2 Modified Scheme. It is mentioned previously that, in the low frequency when the critical frequency $u_0 = 2\pi f_0 d/c < \pi$, energy can be wasted in the invisible region. To avoid this pitfall in the array design, we thus modify Eq. (15) to concentrate the effort on only the visible region $[-u_0, u_0]$. The modified merit factor F_b is written as

$$F_b = \frac{\left(\int_{-u_0}^{u_0} S(u)du\right)^2}{2u_0 \int_{-u_0}^{u_0} [S(u) - \mu_s]^2 du} \quad (17)$$

where

$$\mu_s = \frac{1}{2u_0} \int_{-u_0}^{u_0} S(u)du. \quad (18)$$

Equation (18) can be expressed as

$$\mu_s = \frac{1}{2u_0} \int_{-u_0}^{u_0} \sum_{k=-\infty}^{\infty} [R(k)e^{jku}]du.$$

With some manipulations, above equation can be rewritten as

$$\mu_s = \frac{1}{2u_0} \sum_{k=-\infty}^{\infty} \left[R(k) \frac{2\sin(ku_0)}{k}\right]. \quad (19)$$

Define

$$G_s = \frac{1}{2u_0} \int_{-u_0}^{u_0} S^2(u, f_0)du. \quad (20)$$

From Eqs. (8), (18), and (19), Eq. (20) can be expressed as

$$G_s = \frac{1}{2u_0} \sum_{k=-\infty}^{\infty} \left[C(k) \frac{2\sin(ku_0)}{k}\right]. \quad (21)$$

With some manipulations, the denominator of F_b in Eq. (17) can be written as

$$2u_0 \int_{-u_0}^{u_0} [S(u, f_0) - \mu_s]^2 du = 4u_0^2 G_s - 4u_0^2 \mu_s^2.$$

Equation (17) can now be written as

$$F_b = \frac{\left(\int_{-u_0}^{u_0} S(u, f_0)du\right)^2}{2u_0 \int_{-u_0}^{u_0} [S(u, f_0) - \mu_s]^2 du} = \frac{\mu_s^2}{G_s - \mu_s^2}. \quad (22)$$

4 Genetic Algorithm

The genetic algorithm (GA) is an optimization algorithm based on the theory of biological evolution [8]. The GA is particularly useful for solving complex and nonconvex problems in discrete space with a large number of parameters. The main difference between the GA and other search algorithms is that the GA operates on a "population" of strings (chromosomes) instead of a single starting point. Each chromosome is associated with a "fitness" value as the performance measure. The GA forms "generations" of solution candidates and attempts to maximize the total fitness of each generation. Owing to the multiple-starting-point nature of the algorithm, the GA is less likely to be trapped in a local optimum than many other optimization methods.

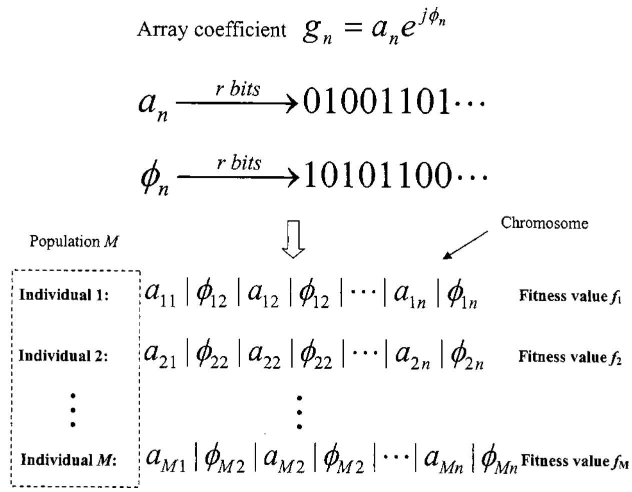

Fig. 4 Binary encoding of array coefficients of GA

4.1 Design Procedure of the GA. The first step of the GA is to encode the input parameters for the fitness function into binary numbers. As shown in Fig. 4, the array coefficients $g_n = a_n e^{j\phi_n}$, $n = -N, -N+1, \ldots, N-1, N$, are encoded in an r-bit discrete space. Then all coefficients are concatenated to form a binary string called a chromosome. The corresponding fitness value is computed.

The flowchart of the array design using GA is shown in Fig. 5. To initialize the GA procedure, M individuals are randomly generated to form the first generation. In a GA cycle, three types of operators are invoked.

Reproduction: Each individual in the current population has a possibility of being selected to form the next generation according to the fitness. The probability to be selected for the kth chromosome is

$$p_k = \frac{f_k - f_{\min}}{\sum_{i=1}^{M} (f_i - f_{\min})} \quad (23)$$

where f_i indicates the fitness function of the ith chromosome and $f_{\min}$ indicates the minimum fitness value in the M chromosomes.

Crossover: With the crossover probability p_c, this step copies data from two parent individuals generated in the previous step to form new child solutions. The method used in this paper is the *doublepoint* crossover, where the two points are randomly chosen, as shown in Fig. 6(*a*). This splits each parent into three segments. The first child solution is formed by randomly copying each segment from either of the parents. The second child solution is formed from the segments not used by the first child. The parents are then replaced by their offsprings.

Mutation: This step is performed on each the chromosome according to the mutation probability p_m by randomly altering chromosomes, as shown in Fig. 6(*b*). The mutation probability p_m

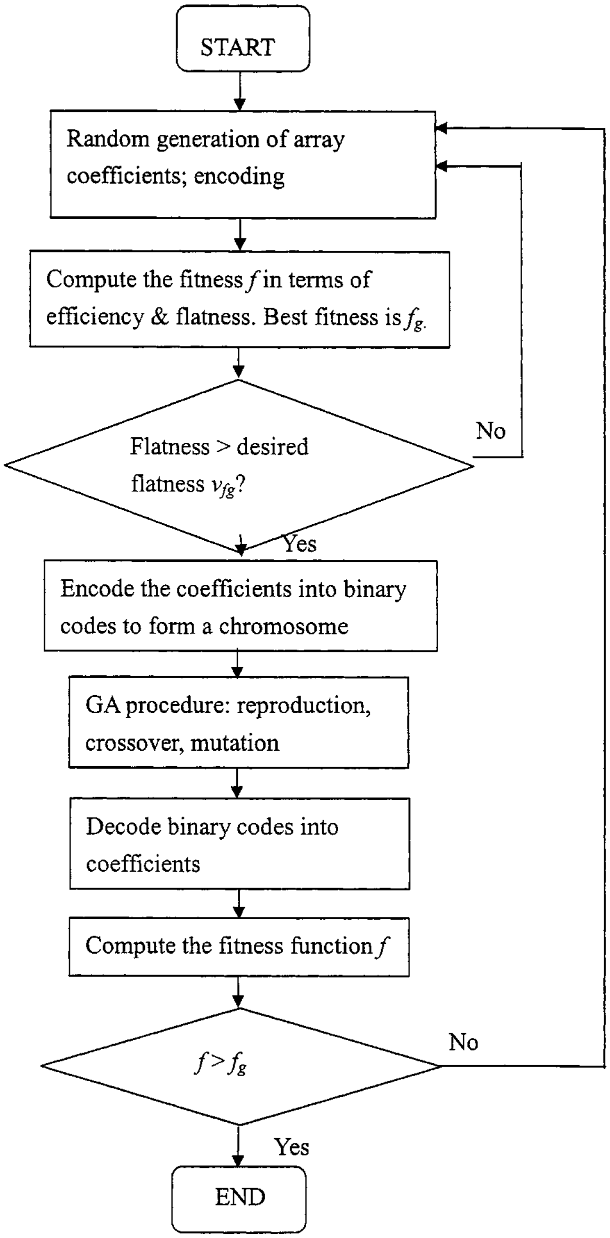

Fig. 5 Flow chart of the GA procedure

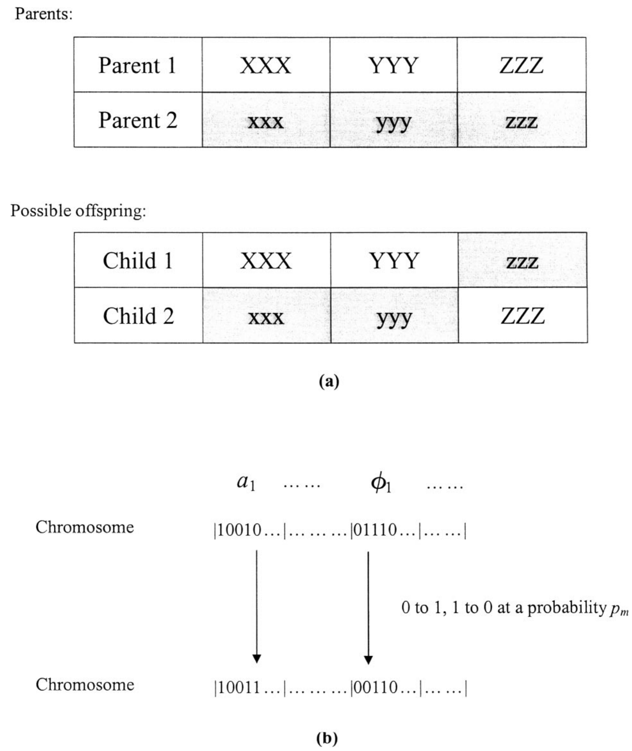

Fig. 6 GA operators (*a*) crossover; (*b*) mutation

must be chosen appropriately. If p_m is too large, the GA will diverge. Conversely, if p_m is too small, the GA will terminate prematurely.

4.2 Application of the GA to the Array Design Problem The parameters for the GA in our array design problem are

$$g_n = a_n e^{j\phi_n}, \quad n = -N, \ldots, N \tag{24}$$

where g_n is a complex constant and a_n, ϕ_n are the magnitude and phase.

First, M sets of array coefficients a_n, ϕ_n are randomly generated. The ranges of the magnitude a_n and the phase ϕ_n are

$$0 \leq a_n \leq 1 \quad \text{and} \quad 0 \leq \phi_n \leq 2\pi.$$

Then, divide the full range into 2^r levels according to the desired resolutions and round the coefficients to the nearest integer. Encode the coefficients a_n and ϕ_n into r-bit binary representations. Then the binary codes of all $2(2N+1)$ coefficients are concatenated to form a chromosome. We note in passing in the GA flowchart of Fig. (5), that the initially generated random numbers have to pass a preliminary screening process based on a threshold of flatness v_{fg} defined in Eq. (16) (the inner loop labeled with "No"). Next, the complete GA cycle involving reproduction, crossover and mutation is applied, under the following constraints, to maximize the merit factor defined in Eq. (14). The GA procedure will repeat itself (the outer loop labeled with "No") until a given target of fitness function, or the merit factor, is met.

4.3 Constraints. In order to ensure uniqueness of solutions, two fundamental constraints must be incorporated into the optimization procedure. The first constraint pertains to the scaling of the array pattern. In order to simplify the formulation, we assume that the gain of the center element is unity.

$$g_0 = 1, \text{ and } |g_k| \leq 1, \text{ where } -N \leq k \leq N, \ k \in N. \tag{25}$$

The second constraint pertains to the "rotation" of the array pattern. To avoid nonunique solutions due to rotation, the following constraint applies

$$\angle g_0 = \angle g_1 = 0. \tag{26}$$

To further simplify the formulation, the magnitudes of the array coefficients are assumed to be symmetric about the center element.

$$|g_{-N}| = |g_N|, |g_{-N+1}| = |g_{N-1}|, \ldots \ldots, |g_{-1}| = |g_1|. \tag{27}$$

Therefore, with these constraints taken into account, the GA procedure is applied to each frequency, resulting in an optimal set of "complex" array coefficients for this frequency. For $f < c/2d$, both schemes can be used, whereas for $f > c/2d$ only the preliminary scheme is required. Let $g_{n,1}, g_{n,2}, \ldots, g_{n,m}$ be the complex array coefficients corresponding to the nth element with respect to the center frequencies f_1, f_2,, f_m. These complex coefficients $g_{n,1}, g_{n,2}, \ldots, g_{n,m}$ serve as the frequency response samples associated with the filter of the nth array element. In order to obtain an array appropriate for real-time processing of broadband signals, we simply applied the inverse fast Fourier transform (IFFT)

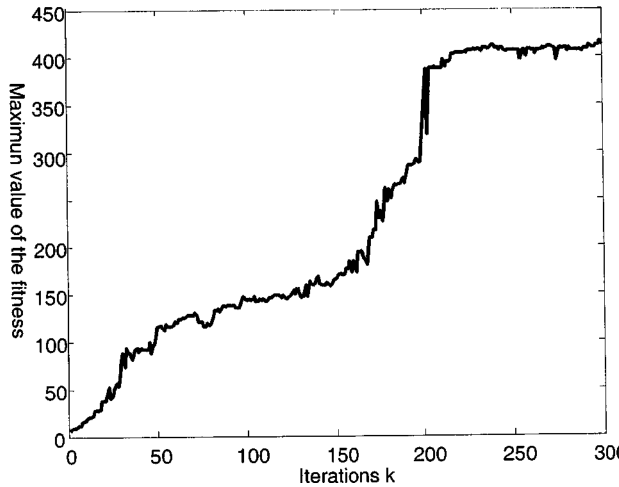

Fig. 7 Learning curve of the fitness function in the GA-based 13×1 array (preliminary scheme)

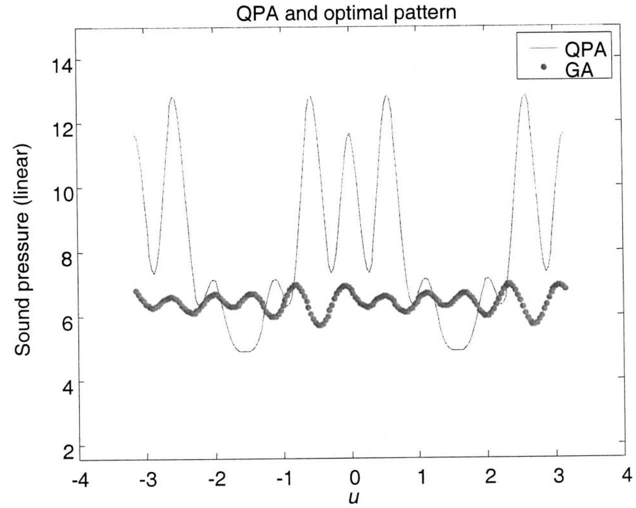

Fig. 8 Comparison of beam patterns between the QPA and the GA (preliminary scheme) at the same efficiency requirement

to calculate the finite impulse response (FIR) filter coefficients for each array element. In this final step, circular shift may be applied to ensure the causality of the resulting filters.

5 Verification of GA-based Array Design

5.1 Numerical Simulation. A simulation was carried out for the omnidirectional array, using the preliminary scheme. With reference to the fitness function, or the merit factor F_a in Eq. (14), we choose $M=200$, $r=16$, and $N=6$ in the simulation. Hence, 6 magnitude parameters and 11 phase parameters of the array elements are arranged into one chromosome. The probabilities of crossover and mutation are set to be 0.85 and 0.01, separately. After approximately 300 iterations through the outer loop labeled with "No" in Fig. 5 (approximately 20 min on a Pentium 3), the fitness function of the GA algorithm settles to the maximum value. The learning curve is shown in Fig. 7 and the results found by GA are summarized in Table I. Figure 8 compares the beam pattern $|B(u)|$ obtained by the GA with the beam pattern obtained by the quadratic phase array (QPA) [5]. It can be seen from the result that the GA design that is based on the procedure in Fig. 5 with the merit factor of Eq. (14) produced a flatter array pattern than the QPA design.

Next, the modified scheme is investigated. The fitness function, or the merit factor F_b in Eq. (22), is used in the GA procedure. Choose $u_0=1.5$ and $N=2$ in the optimization program. Simulated beam pattern using optimal array coefficients is shown in Fig. 9.

Table 1 The array coefficients for the 13×1 optimal array (preliminary scheme) and the QPA array

Element index	Optimal array	QPA ($z=18$)
−6	0.13 exp(j0.72)	0.74
−5	0.52 exp(−j2.64)	−0.78
−4	0.64 exp(−j0.29)	0.96
−3	0.53 exp(j1.80)	−1.00
−2	1.00 exp(−j1.81)	0.45
−1	0.87 exp(j0.78)	0.67
0	1	−0.86
1	0.87	−0.67
2	1.00 exp(j1.81)	0.45
3	0.53 exp(j1.34)	1.00
4	0.64 exp(j0.29)	0.96
5	0.52 exp(−j0.50)	0.78
6	0.13 exp(−j0.72)	0.74
Efficiency	0.63	0.63
Flatness	0.12	5.95

Using the modified scheme, we are able to concentrate the beam pattern in the visible region, $u=-1.5\sim1.5$. This enhancement of efficiency is obtained for the frequency

$$f<\frac{u_0c}{2\pi d}. \tag{28}$$

For a frequency 1123 Hz satisfying the above relation, we compare the beam patterns between the two designs using the preliminary scheme and the modified scheme, respectively. The spacing $d=6.7$ cm. The results in Fig. 10 show that the array using the modified scheme gives larger output than the array using the preliminary scheme.

5.2 Experimental Investigation. A small 5×1 linear panel speaker array and a large 3×3 panel speaker matrix are constructed for experimental verification. The dimensions of the small panels are 7 cm×6.7 cm and the dimensions of the large panels are 30 cm×30 cm. The spacing d is 6.7 cm in the 5×1 array and 30 cm in the 3×3 matrix. The resulting designs are implemented on a digital signal processor (DSP) platform. All measurements were conducted inside a 3 m×3 m×4 m anechoic chamber.

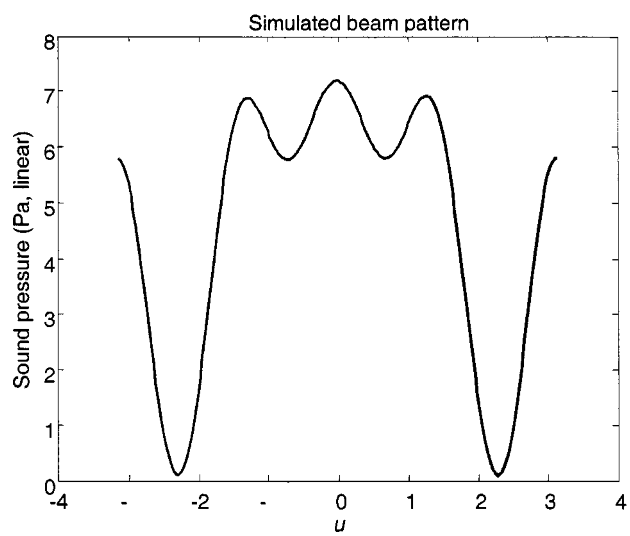

Fig. 9 Beam pattern obtained using the modified scheme, plotted against the dimensionless angle

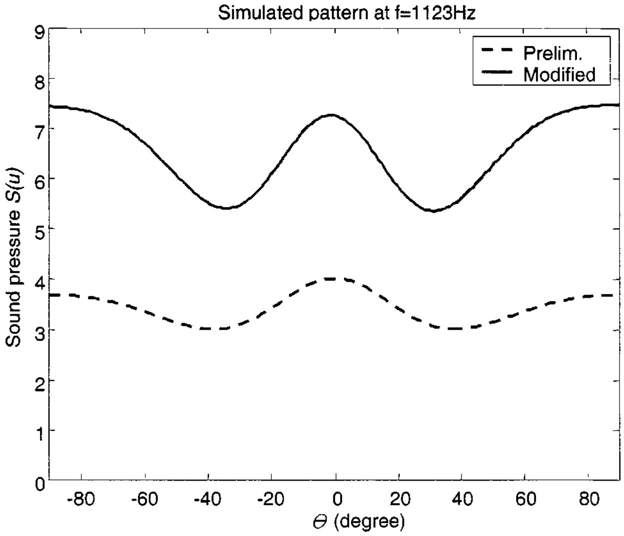

Fig. 10 Comparison of beam patterns between the two designs using the preliminary scheme and the modified scheme, respectively. The frequency is 1123 Hz, and the spacing $d=6.7$ cm

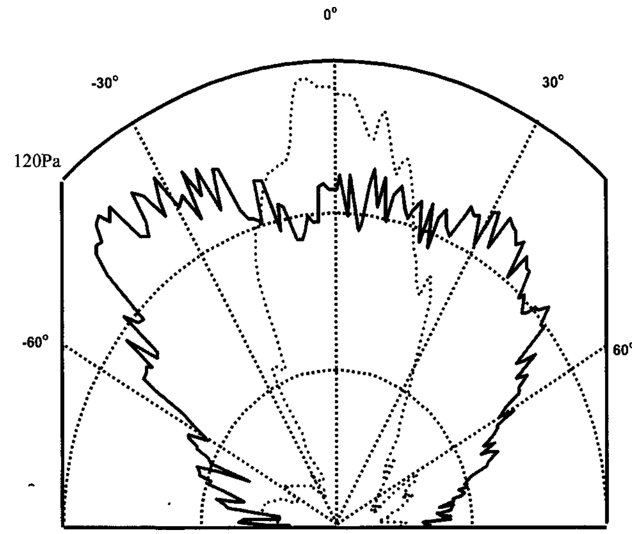

Fig. 12 Measured beam pattern of the 3×3 panel speaker matrix in the frequency 1514 Hz. The array is designed using the preliminary scheme of the GA procedure (dashed line: uncompensated; solid line: compensated using the GA design)

The first experiment pertains to the verification of the array design using the preliminary scheme of the GA procedure. Figure 11 shows the measured beam pattern of the 5×1 panel speaker array at the frequency 3 kHz. Figure 12 shows the measured beam pattern of the 3×3 panel speaker matrix at the frequency 1514 Hz. The results of these two figures indicated that the compensated array resulting from the modified GA design exhibits omnidirectional characteristics within the angles approximately from -60 deg to 60 deg.

The second experiment pertains to the verification of the array design using the modified scheme of the GA procedure. Figure 13 shows the measured beam pattern of the 5×1 panel speaker array at the frequency 1134 Hz. Figure 14 shows the measured beam pattern of the 3×3 panel speaker matrix at the frequency 879 Hz. From the experimental results, it is observed that the modified scheme of GA procedure indeed produced a design with a higher output level than the preliminary scheme.

6 Conclusions

It has been illustrated in this work that an omnidirectional radiation pattern of panel speaker array can be achieved by using the GA-based optimization method. Both numerical and experimental investigations are carried out to justify the proposed techniques. A preliminary scheme and a modified scheme were developed to maximize the array efficiency under desired spectral flatness requirement. The GA proved to be an effective search technique for the current array design problem. In particular, the modified scheme is able to enhance the efficiency in frequency $f<c/2d$. The proposed GA procedure generally yields a satisfactory design with a short computational time. For the broadband case, both schemes can be combined to deal with different frequency ranges.

The resulting optimal designs are implemented on a DSP platform and are experimentally verified by using a small 5×1 panel speaker array and a large 3×3 panel speaker array. The experi-

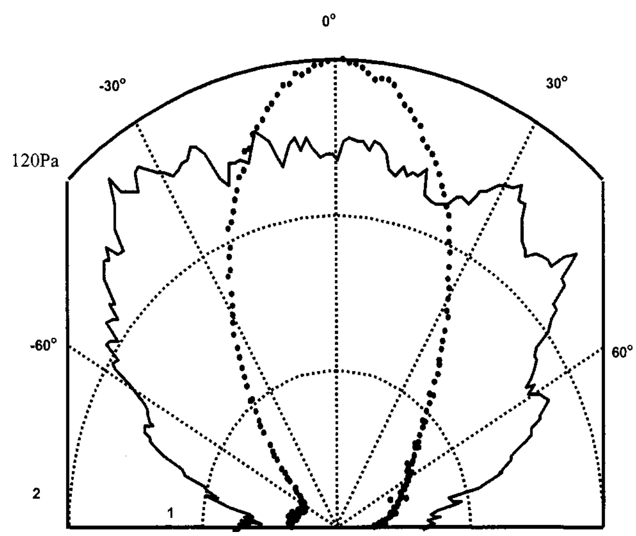

Fig. 11 Measured beam pattern of the 5×1 panel speaker array in the frequency 3 kHz. The array is designed using the preliminary scheme of the GA procedure (dashed line: uncompensated; solid line: compensated using the GA design)

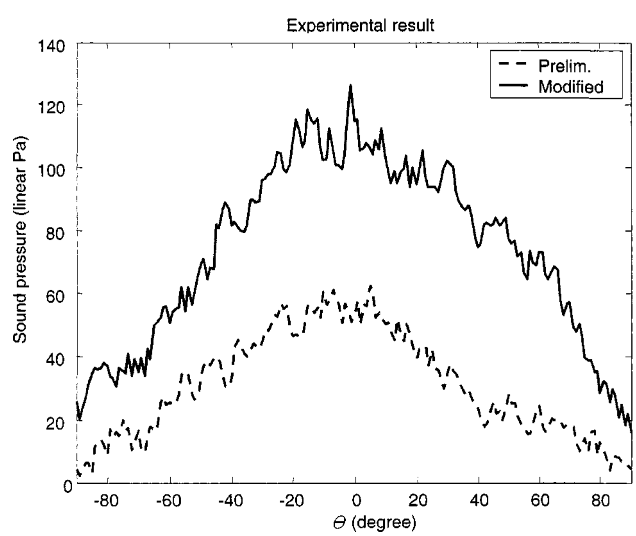

Fig. 13 Measured beam patterns of the 5×1 panel speaker array in the frequency 1123 Hz (dashed line: preliminary scheme; solid line: modified scheme)

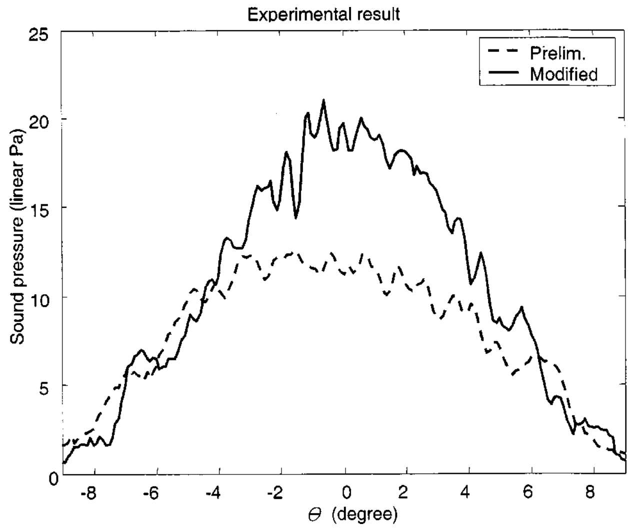

Fig. 14 Measured beam patterns of the 3×3 panel speaker matrix in the frequency 879 Hz (dashed line: preliminary scheme; solid line: modified scheme)

mental results indicate that the proposed GA techniques are able to produce an array design with an omnidirectional beam pattern. Between the two designs, the modified scheme yields more output by shifting the effort from the invisible region to the visible.

Although the ultimate goal of this work was to develop the large array, we were unable to verify its far-field behavior due to the limitation of current measuring environment. Much work is continuing in improving the implementation as well as measurement of the large array for future research.

Acknowledgments

Special thanks are due to the illuminating discussions with NXT, New Transducers Limited, UK. The work was supported by the National Science Council in Taiwan, under the Project No. NSC 89AFA06000714.

References

[1] Bai, M. R., and Huang, T., 2001, "Development of Panel Loudspeaker System: Design, Evaluation and Enhancement," J. Acoust. Soc. Am., **109**, pp. 2751–2761.
[2] Johnson, D. F., and Dudgeon, D. F., 1993, *Array Signal Processing Concepts and Techniques* Prentice Hall, Englewood Cliffs, NJ.
[3] Haupt, R. L., 1994, "Thinned Arrays Using Genetic Algorithms," IEEE Trans. Antennas Propag., **42**, pp. 993–999.
[4] Smith, D. L., 1997, "Discrete-Element Line Arrays: Their Modeling and Optimization," J. Audio Eng. Soc., **45**, pp. 949–964.
[5] Aarts, R. M., and Janssen, A. J. E. M., 2000, "On Analytic Design of Loudspeaker Arrays with Uniform Radiation Characteristics," J. Acoust. Soc. Am., **107**, pp. 287–292.
[6] Beenker, G. F. M., Claasen, T. A. C. M., and Hermens, P. W. C., 1985, "Binary Sequences With a Maximally Flat Amplitude Spectrum," Philips J. Res., **40**, pp. 289–304.
[7] Golay, M. J. E., 1982, "The Merit Factor of Long, Low Autocorrelation Binary Sequences," IEEE Trans. Inf. Theory, **28**, pp. 543.
[8] Belew, R. K., and Vose, M. D., 1997, *Foundations of Genetic Algorithms*, Morgan Kaufmann Publishers, New York.
[9] Augspurger, G. L., 1990, "Near-Field and Far-Field Performance of Large Woofer Arrays," J. Audio Eng. Soc., **38**, pp. 231–236.
[10] Meyer, D. G., 1984, "Digital Control of Loudspeaker Array Directivity," J. Audio Eng. Soc., **32**, pp. 747–754.
[11] Oppenheim, A. V., and Schafer, R. W., 1989, *Discrete-Time Signal Processing*, Prentice Hall, Englewood Cliffs, NJ.